Hindawi Publishing Corporation
International Journal of Photoenergy
Volume 2012, Article ID 927132, 6 pages
doi:10.1155/2012/927132

Research Article

Photocatalytic Degradation of Rhodamine B with $H_3PW_{12}O_{40}/SiO_2$ Sensitized by H_2O_2

Shuijin Yang, Yongkui Huang, Yunzhi Wang, Yun Yang, Mingbo Xu, and Guohong Wang

Hubei Key Laboratory of Pollutant Analysis & Reuse Technology, College of Chemistry and Environmental Engineering, Hubei Normal University, Huangshi 435002, China

Correspondence should be addressed to Guohong Wang, wanggh2003@163.com

Received 25 July 2012; Accepted 31 August 2012

Academic Editor: Huogen Yu

In order to remove aquatic organic dye contaminants by utilizing the inexpensive and inexhaustible solar energy, the Keggin-type $H_3PW_{12}O_{40}$ was loaded on the surface of SiO_2 with the sol-gel method and sensitized by H_2O_2 solution. The photocatalytic degradation of rhodamine B (RhB) by $H_3PW_{12}O_{40}/SiO_2(x)$ under simulated natural light irradiation was investigated. The effects of the initial RhB concentration, the solution pH, and catalyst dosage on the photocatalytic degradation rate of RhB were also studied. The results demonstrated that at optimal condition (initial concentration of methyl orange is 10 mg/L, catalyst dosage is 0.8 g, and the pH is 2.5) the degradation rate of RhB is as high as 97.7% after 2 h under simulated natural light irradiation. The reaction of photocatalysis for RhB can be expressed as a first-order kinetic model.

1. Introduction

Environmental pollution caused by organic dyes has become a worldwide problem. Those dyes are often used in textiles, papers, leathers, food, and cosmetics. It is essential to develop methods that can lead to destruction of such compounds. A variety of common treatment techniques including condensation, ultrafiltration, membrane separation, and adsorption have become the main technology for treatment of organic pollutants [1, 2]. However, these methods often transferred organic pollutants to the other phases and not degraded completely to nontoxic substances [3–5]. So, the development of advanced low cost and high efficiency water treatment technologies is desirable.

Advanced oxidation processes (AOPs) in organic pollutants degradation have shown outstanding advantages, which have the potential to completely oxidize organic compounds to CO_2, H_2O, and other inorganic substances [6–8]. Among these AOPs, photocatalytic degradation by semiconductor catalysts has been investigated widely during the past decade. A number of semiconductor materials such as TiO_2 [9, 10], ZnO [11], Fe_2O_3 [12], Bi_2WO_6 [13], $H_2WO_4 \cdot H_2O/Ag/AgCl$ [14], Ag_2O [15], and $SrTiO_3$ [16] were used in photocatalytic degradation of organic pollutants. Among them, the use of TiO_2 as a photocatalyst to degrade organic pollutants has recieved extensive attention due to its high activity, low cost, chemical stability, and nontoxicity [17, 18]. But this photocatalyst is activated only by ultraviolet (UV) light (wavelength < 387 nm) due to its band gap of 3.2 eV. Since UV light only accounts for less than 5% of the solar energy that reaches the surface of the earth, the photocatalytic activity of pure TiO_2 cannot be effectively activated under solar light irradiation, which limits its practical application [19, 20].

In recent years, the development of photocatalysts with a visible light response has been extensively studied. For this purpose, TiO_2 has been modified by various ways such as impurity doping inorganic compound [21, 22] and dye sensitization [23] to obtain visible light reactivity [24, 25]. Polyoxometalates (POMs) have also attracted much attention as photocatalysts because they generally share the same photochemical characteristics of semiconductor photocatalysts such as TiO_2 [26, 27]. The excited POMs, produced after light absorption is able to completely degrade organic compounds, either directly or via OH radicals-mediated oxidations [28]. A problem of POMs catalysts used to degrade pollutants in homogeneous systems is that they are difficult to separate from the reaction system at the end of the reaction,

which precludes their recovery and reuse. POMs should be supported on a support to improve the catalytic performance in the reaction [29]. SiO_2 was an ideal support because it exhibits higher surface area, chemical inertness, controlled porosity and well disperses for POMs while retaining the structure. Unfortunately, the photocatalysis of POMs/SiO_2 are concentrated on UV irradiation [30]. Aiming at utilizing the inexpensive and inexhaustible solar energy, we attempted to use a simple and efficient method to improve their photocatalytic activity.

In this paper, $H_3PW_{12}O_{40}/SiO_2$ was prepared by a sol-gel technique, and sensitized by H_2O_2 solution. The photocatalytic degradation of RhB with the catalyst under simulated natural light irradiation was investigated.

2. Experimental

2.1. Preparation of Samples. $H_3PW_{12}O_{40}/SiO_2$ was synthesized according to references [26, 30] by a sol-gel technique. An amount of $H_3PW_{12}O_{40}$ was dissolved in 26 mL of H_2O, and a stoichiometric amount of TEOS was mixed with 1-BuOH. The latter was added dropwise to the aqueous solution. The resultant was allowed to stir at room temperature for 1 h, at 45°C for 1 h, and then at 80°C until a uniform gel was formed. The hydrogel obtained was dehydrated slowly at 45°C for 16 h in vacuum, and then at 90°C for 3.5 h. Thus, the silica network was fastened and the removal of the $H_3PW_{12}O_{40}$ molecules from it was avoided. The particulate gel was washed with hot water for several times until the filtrate was neutral, and then the products were calcined for the required duration. The acetalization of cyclohexanone with 1, 2-propanediol was used as a probe to study the preparation conditions of catalyst, and the optimum conditions are as follows the loading of $H_3PW_{12}O_{40}$ is 30 wt% calcination temperature is 200°C; and calcination time is 4 h.

$H_3PW_{12}O_{40}/SiO_2$ was treated by H_2O_2 as follows [17]: 1 g $H_3PW_{12}O_{40}/SiO_2$was added into 15 mL 30% H_2O_2 solution and sonicated the mixture for 20 min. The slurry mixture was filtrated and dried at room temperature. This catalyst is denoted as $H_3PW_{12}O_{40}/SiO_2$(x).

2.2. Characterization. The FT-IR spectra of the samples in KBr matrix were recorded on a Nicolet 5700 FT-IR spectrometer in the range 400–4000 cm^{-1}. The X-ray powder diffraction pattern of the samples was measured by a Bruker AXS D8-Advanced diffractometer (Bruker, Germany) employing Cu K_α radiation. The UV-vis diffuse reflectance spectra (UV-vis/DRS) were recorded on a spectrophotometer with an integrating sphere (Shmadzu UV-2550), and $BaSO_4$ was used as a reference sample.

2.3. Activity Test. For the evaluation of catalyst activity, the catalyst was suspended in an aqueous solution of rhodamine B (RhB) in a Pyrex reactor. The photoreactor was designed with a light source surrounded by a quartz jacket. Simulated sunlight irradiation was provided by a 500 W xenon lamp (Nanjing Xujiang Electromechanical Factory, China), and the intensity of the lamp was 1200 $\mu mol \cdot m^{-2} \cdot s^{-1}$. Solution pH was adjusted with dilute aqueous HCl and NaOH solutions. The system was cooled by circulating water and maintained at room temperature. Before irradiation, the suspensions were magnetically stirred in the dark for 30 min to reach the adsorption–desorption equilibrium of organic dyes on catalyst surface. At given time intervals, about 3 mL suspension was continually taken from the photoreactor for subsequent RhB concentration analysis after centrifuging. Decreases of the RhB concentrations were monitored via a UV-visible spectrometer (Hitachi U-3010, Japan). The degradation yield of organics was calculated by the following formula:

$$\text{degradation yield (\%)} = \left(\frac{(A_0 - A)}{A_0}\right) \times 100, \quad (1)$$

where A_0 and A referred to the absorbance of RhB before and after reaction, respectively.

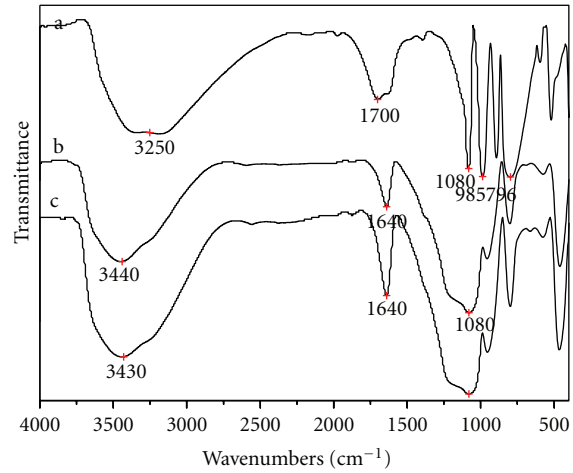

FIGURE 1: FT-IR spectra of $H_3PW_{12}O_{40}$ (a), $H_3PW_{12}O_{40}/SiO_2$ (b), and $H_3PW_{12}O_{40}/SiO_2$(x) (c).

3. Results and Discussion

3.1. Characterization of the Catalysts. The FT-IR spectra of $H_3PW_{12}O_{40}$ (a), $H_3PW_{12}O_{40}/SiO_2$ (b), and $H_3PW_{12}O_{40}/SiO_2$(x) (c) are shown in Figure 1. As shown in Figure 1, pure $H_3PW_{12}O_{40}$ gives peaks due to the Keggin structure at 1080, 985, 890, and 794 cm^{-1}. In addition, the band at 1662 cm^{-1}, which is the bending mode of the water, indicates the presence of the water. When $H_3PW_{12}O_{40}$ is supported on SiO_2, these bands have somewhat changed. The bands at 1080 and 890 cm^{-1} are overlapped by the characteristic band of SiO_2, while these bands at 985 and 794 cm^{-1} shift to 950 and 803 cm^{-1}, respectively. The spectrum of $H_3PW_{12}O_{40}/SiO_2$(x) is similar to that of $H_3PW_{12}O_{40}/SiO_2$. It can be concluded that the Keggin geometry of $H_3PW_{12}O_{40}$ is still kept [31]. Meanwhile, it indicates that a strong chemical interaction exists between the $H_3PW_{12}O_{40}$ and silica.

POMs could be supported as molecules or aggregates on the supports. Figure 2 shows the X-ray diffraction patterns of $H_3PW_{12}O_{40}$ (a), $H_3PW_{12}O_{40}/SiO_2$ (b), and $H_3PW_{12}O_{40}/SiO_2$(x) (c). The characteristic diffraction peaks of $H_3PW_{12}O_{40}$ at 8–10°, 17–20°, 26–30°, and 32–35° can be

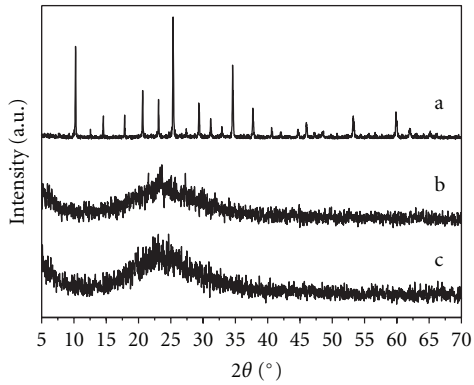

Figure 2: XRD patterns of $H_3PW_{12}O_{40}$ (a), $H_3PW_{12}O_{40}/SiO_2$(b), and $H_3PW_{12}O_{40}/SiO_2$(x) (c).

assigned to the diffraction characteristic peaks of crystalline $H_3PW_{12}O_{40}$ Keggin structure [31]. For $H_3PW_{12}O_{40}/SiO_2$ and $H_3PW_{12}O_{40}/SiO_2$(x), only a broad band at $2\theta = 24°$ that can be assigned to the diffraction peaks of amorphous silica is observed, and the signals of $H_3PW_{12}O_{40}$ are disappeared. So it is reasonable to consider that $H_3PW_{12}O_{40}$ is highly dispersed on the surface of silica support without any aggregation.

The diffusing reflectance UV-Vis spectra (UV-DRS) of the catalysts are directly related to their photochemical behavior. The UV-DRS of the samples were characterized, and the results are shown in Figure 3. From the Figure 3, it can be seen clearly the characteristic absorption peaks at 260 nm which was attributed to O-W charge transfer of the Keggin unit at W-O-W bond. Their characteristics are similar to pure $H_3PW_{12}O_{40}$.This can be assigned to the Keggin geometry of $H_3PW_{12}O_{40}$ [31]. It is worthy to note that an absorption tail extending from the UV to the visible region in the UV-DRS of $H_3PW_{12}O_{40}/SiO_2$(x). Therefore, it is concluded that the sensitizing effect maybe have obvious influence on the photocatalytic activity of catalyst.

3.2. Investigation of Photocatalytic Activity of Catalysts

3.2.1. Comparison of Photocatalytic Activity of Catalysts. In order to observe the effect of H_2O_2 treatment on the catalytic activity of $H_3PW_{12}O_{40}/SiO_2$, comparison of photocatalytic activity of catalysts was carried out at the initial RhB concentration of 10 mg/L, pH 2.5, and 0.5 g of catalyst, and the results are shown in Figure 4.

As seen from Figure 4, after 2 h irradiation under the same conditions, no obvious RhB degradation was observed without any catalyst or light. However, in the presence of $H_3PW_{12}O_{40}/SiO_2$, the degradation yield of RhB is about 44.0%, while with $H_3PW_{12}O_{40}/SiO_2$(x) the degradation yield can reach to 92.7%. Since the $H_3PW_{12}O_{40}/SiO_2$ is illuminated by ultraviolet light, which represents 3 to 5% of the total solar radiation. This is consistent with previous reports [26, 30]. So the photodegradation reaction of RhB in the presence of $H_3PW_{12}O_{40}/SiO_2$(x) is more effectively than that of $H_3PW_{12}O_{40}/SiO_2$.

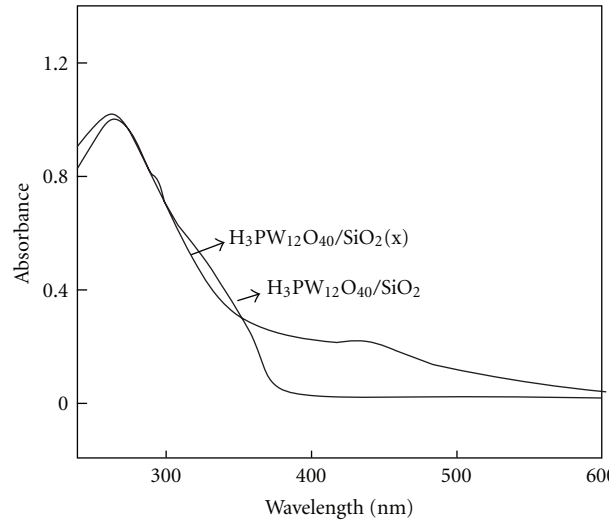

Figure 3: UV-vis/DRS of $H_3PW_{12}O_{40}/SiO_2$ and $H_3PW_{12}O_{40}/SiO_2$(x).

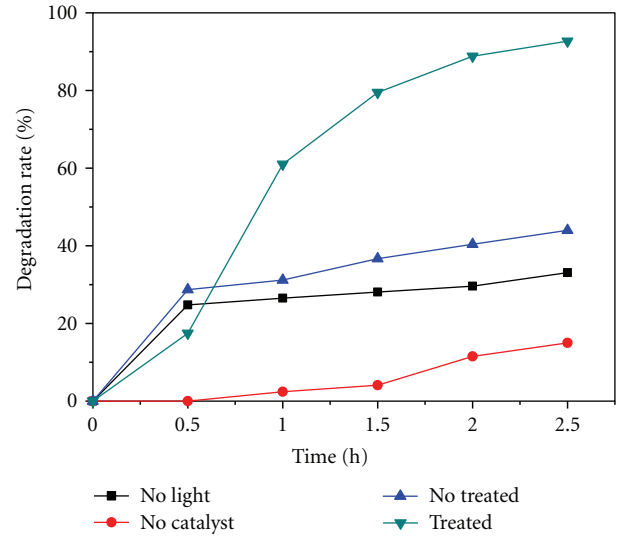

Figure 4: Comparison of photocatalytic activity before and after treatment of catalysts, and under no light or without catalyst.

3.2.2. Effect of the Initial Concentration of Dye. To investigate the influence of initial concentration on the degradation efficiency of RhB, the initial concentration was varied from 5 to 20 mg/L, keeping the other experimental conditions constant.

As can be seen in Figure 5, the degradation rate decreased with increase of initial concentration of RhB. This might be due to the excessive adsorption of the RhB molecules on the surface of catalyst at higher concentration. Moreover, light through the solution is reduced significantly. Thus, the efficiency of degradation was decreased in the higher concentration. It was further observed that the activity decreased slightly from 5 to 10 mg/L of the initial concentration of dye. From the practical point of wastewater treatment, the initial concentration of the 10 mg/L is more appropriate.

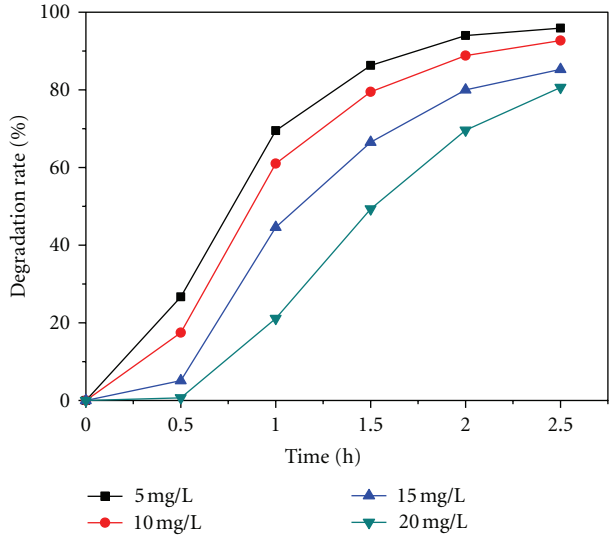

Figure 5: Effect of the initial RhB concentration on the photocatalytic degradation rate of RhB.

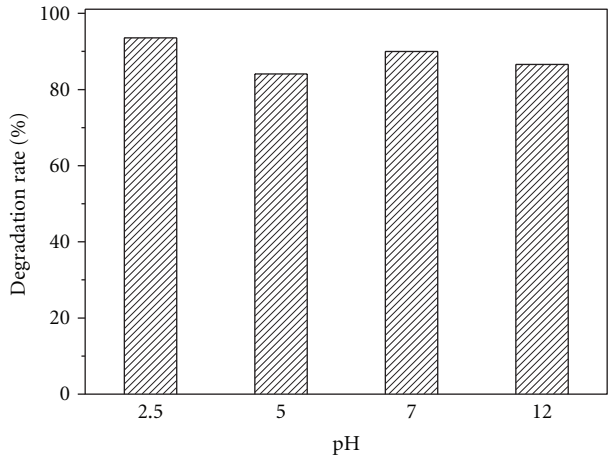

Figure 6: Effect of the solution pH on the photocatalytic degradation rate of RhB.

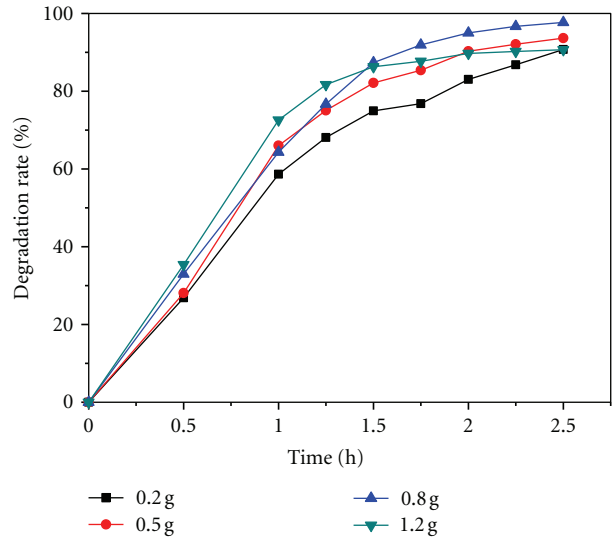

Figure 7: Effect of catalyst dosage on the photocatalytic degradation rate of RhB.

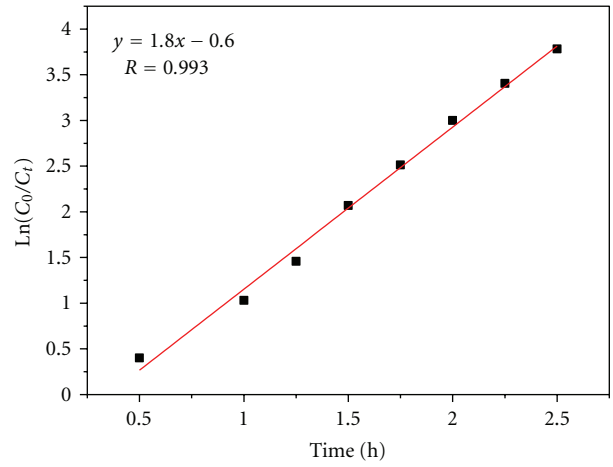

Figure 8: Relation curve of $\ln(C_0/C_t)$ and time (t).

3.2.3. Effect of pH. It is well known that the pH of the solution is one of the most important parameters in the photocatalytic degradation of organic compounds. This is attributed to that the pH does not only determine chemical properties of the photocatalyst but also influences adsorption behaviour of the pollutants. Therefore, the effect of pH on the degradation of RhB was studied at pH range from 2.5 to 12.

As shown in Figure 6, the most effective pH condition is at 2.5. This may be ascribed to the fact that the pH value could influence the amount of hydroxyl radicals (OH·) formed [21] and the stable of $H_3PW_{12}O_{40}$. So the optimum pH of the solution is 2.5.

3.2.4. Effect of Catalyst Dosage. The catalyst dosage is also an important parameter for optimizing the operational conditions. Therefore, the effect of catalyst dosage on the degradation of RhB was investigated in the catalyst dosage from 0.2 to 1.2 g, and the result shown was in Figure 7. The results indicated that the degradation rate gradually increased with increase of catalyst dosage from 0.2 to 0.8 g. However, the degradation efficiency decreased slightly with increase of catalyst dosage from 0.8 to 1.2 g. This may be attributed to the fact that the surplus catalyst can scatter the photons in the photoreaction system.

3.3. Kinetic Analysis. It is well known that the photodegradation of organic dyes mainly follows first-order kinetics. The kinetics of photocatalytic degradation of RhB was also studied under optimized conditions. The results are shown in Figure 8.

The results showed that the photocatalytic degradation of RhB over $H_3PW_{12}O_{40}/SiO_2$ (x) under simulated sunlight irradiation can be described by the first order kinetic model, $\ln(C_0/C_t) = kt$, where k is the rate constant (h^{-1}), C_0 is

the initial concentration, and C_t is the concentration of dye at time t. It can be seen for Figure 8 that the plots represented a straight line. The correlation constant for the line was 0.993. The rate constant was $1.8\,h^{-1}$.

4. Conclusion

$H_3PW_{12}O_{40}/SiO_2$was prepared by a sol-gel method and sensitized by H_2O_2 solution and significantly improved its catalytic activity under simulated natural light irradiation. The photocatalytic degradation of RhB by $H_3PW_{12}O_{40}/SiO_2$ (x) under simulated natural light irradiation was investigated. The results demonstrated that at optimal condition (initial concentration of methyl orange is 10 mg/L, catalyst dosage is 0.8 g, and the pH is 2.5), the degradation rate of RhB is as high as 97.7% after 2 h under simulated natural light irradiation. The reaction of photocatalysis for RhB can be expressed as first-order kinetic model.

Acknowledgments

This work was financially supported by the Young and Middle-Aged Natural Science Foundation of Hubei Province Education Department (no. Q20112507 and, Q20082202) and Hubei Key Laboratory of Pollutant Analysis & Reuse Technology (no. KY2010G13).

References

[1] F. H. Hussein, "Comparison between solar and artificial photocatalytic decolorization of textile industrial wastewater," *International Journal of Photoenergy*, vol. 2012, Article ID 793648, 10 pages, 2012.

[2] M. N. Chong, B. Jin, C. W. K. Chow, and C. Saint, "Recent developments in photocatalytic water treatment technology: a review," *Water Research*, vol. 44, no. 10, pp. 2997–3027, 2010.

[3] M. Muruganandham and M. Swaminathan, "Decolourisation of reactive orange 4 by fenton and photo-Fenton oxidation technology," *Dyes and Pigments*, vol. 63, no. 3, pp. 315–321, 2004.

[4] E. Sahinkaya, N. Uzal, U. Yetis, and F. B. Dilek, "Biological treatment and nanofiltration of denim textile wastewater for reuse," *Journal of Hazardous Materials*, vol. 153, no. 3, pp. 1142–1148, 2008.

[5] H. Lachheb, E. Puzenat, A. Houas et al., "Photocatalytic degradation of various types of dyes (Alizarin S, Crocein Orange G, Methyl Red, Congo Red, Methylene Blue) in water by UV-irradiated titania," *Applied Catalysis B*, vol. 39, no. 1, pp. 75–90, 2002.

[6] S. H. S. Chan, T. Y. Wu, J. C. Juan, and C. Y. Teh, "Recent developments of metal oxide semiconductors as photocatalysts in advanced oxidation processes (AOPs) for treatment of dye waste-water," *Journal of Chemical Technology & Biotechnology*, vol. 86, no. 9, pp. 1130–1158, 2011.

[7] C. C. Hsueh and B. Y. Chen, "Comparative study on reaction selectivity of azo dye decolorization by Pseudomonas luteola," *Journal of Hazardous Materials*, vol. 141, no. 3, pp. 842–849, 2007.

[8] C. McCullagh, N. Skillen, M. Adams, and P. K. Robertson, "Photocatalytic reactors for environmental remediation: a review," *Journal of Chemical Technology & Biotechnology*, vol. 86, no. 8, pp. 1002–1017, 2011.

[9] M. Y. Guo, A. M. C. Ng, F. Liu, A. B. Djurišić, and W. K. Chan, "Photocatalytic activity of metal oxides-the role of holes and OH radicals," *Applied Catalysis B*, vol. 107, no. 1-2, pp. 150–157, 2011.

[10] L. N. Wang, F. Lu, and F. M. Meng, "Synthesis and photocatalytic activity of TiOX powders with different oxygen defects," *International Journal of Photoenergy*, vol. 2012, Article ID 208987, 7 pages, 2012.

[11] J. Fenoll, P. Hellín, C. M. Martínez et al., "Semiconductor oxides-sensitized photodegradation of fenamiphos in leaching water under natural sunlight," *Applied Catalysis B*, vol. 115-116, pp. 31–37, 2012.

[12] X. M. Zhou, J. Y. Lan, G. Liu et al., "Facet-mediated photodegradation of organic dye over hematite architectures by visible light," *Angewandte Chemie*, vol. 124, no. 1, pp. 182–186, 2012.

[13] H. G. Yu, R. Liu, X. F. Wang et al., "Enhanced visible-light photocatalytic activity of Bi_2WO_6 nanoparticles by Ag_2O cocatalyst," *Applied Catalysis B*, vol. 111-112, pp. 326–333, 2012.

[14] X. F. Wang, S. F. Li, Y. Q. Ma, H. Yu, and J. Yu, "$H_2WO_4 \bullet H_2O$/Ag/AgCl composite nanoplates: a plasmonic Z-scheme visible-light photocatalyst," *Journal of Physical Chemistry C*, vol. 115, no. 30, pp. 14648–14655, 2011.

[15] X. F. Wang, S. F. Li, H. G. Yu et al., "Ag_2O as a new visible-light photocatalyst: self-stability and high photocatalytic activity," *Chemistry*, vol. 17, no. 28, pp. 7777–7780, 2011.

[16] X. Wei, G. Xu, Z. Ren et al., "Single-crystal-like mesoporous $SrTiO_3$ spheres with enhanced photocatalytic performance," *Journal of the American Ceramic Society*, vol. 93, no. 5, pp. 1297–1305, 2010.

[17] J. Zou, J. Gao, and Y. Wang, "Synthesis of highly active H_2O_2-sensitized sulfated titania nanoparticles with a response to visible light," *Journal of Photochemistry and Photobiology A*, vol. 202, no. 2-3, pp. 128–135, 2009.

[18] S. Yanagida, A. Nakajima, T. Sasaki, T. Isobe, Y. Kameshima, and K. Okada, "Preparation and photocatalytic activity of Keggin-ion tungstate and TiO_2 hybrid layer-by-layer film composites," *Applied Catalysis A*, vol. 366, no. 1, pp. 148–153, 2009.

[19] Q. J. Xiang, J. G. Yu, and M. Jaroniec, "Graphene-based semiconductor photocatalysts," *Chemical Society Reviews*, vol. 41, pp. 782–796, 2012.

[20] Q. Zhang, D. Q. Lima, I. Lee, F. Zaera, M. Chi, and Y. Yin, "A highly active titanium dioxide based visible-light photocatalyst with nonmetal doping and plasmonic metal decoration," *Angewandte Chemie*, vol. 50, no. 31, pp. 7088–7092, 2011.

[21] Q. J. Xiang, J. G. Yu, W. G. Wang, and M. Jaroniec, "Nitrogen self-doped nanosized TiO_2 sheets with exposed 001 facets for enhanced visible-light photocatalytic activity," *Chemical Communications*, vol. 47, no. 24, pp. 6906–6908, 2011.

[22] Z. H. Xu and J. G. Yu, "Visible-light-induced photoelectrochemical behaviors of Fe-modified TiO_2 nanotube arrays," *Nanoscale*, vol. 3, pp. 3138–3144, 2011.

[23] J. G. Yu, J. J. Fan, and B. Cheng, "Dye-sensitized solar cells based on anatase TiO_2 hollow spheres/carbon nanotube composite films," *Journal of Power Sources*, vol. 196, no. 18, pp. 7891–7898, 2011.

[24] H. R. Jafry, M. V. Liga, Q. Li, and A. R. Barron, "Simple route to enhanced photocatalytic activity of P 25 titanium dioxide nanoparticles by silica addition," *Environmental Science & Technology*, vol. 45, no. 4, pp. 1563–1568, 2011.

[25] H. Li, D. Wang, P. Wang, H. Fan, and T. Xie, "Synthesis and studies of the visible-light photocatalytic properties of near-monodisperse Bi-doped TiO_2 nanospheres," *Chemistry*, vol. 15, no. 45, pp. 12521–12527, 2009.

[26] Y. H. Guo and C. W. Hu, "Heterogeneous photocatalysis by solid polyoxometalates," *Journal of Molecular Catalysis A*, vol. 262, no. 1-2, pp. 136–148, 2007.

[27] P. X. Lei, C. C. Chen, J. Yang, W. Ma, J. Zhao, and L. Zang, "Degradation of dye pollutants by immobilized polyoxometalate with H_2O_2 under visible-light irradiation," *Environmental Science & Technology*, vol. 39, no. 21, pp. 8466–8474, 2005.

[28] I. Arslan-Alaton, "Homogenous photocatalytic degradation of a disperse dye and its dye bath analogue by silicadodecatungstic acid," *Dyes and Pigments*, vol. 60, no. 2, pp. 167–176, 2004.

[29] S. J. Jiang, Y. H. Guo, C. H. Wang, X. Qu, and L. Li, "One-step sol-gel preparation and enhanced photocatalytic activity of porous polyoxometalate-tantalum pentoxide nanocomposites," *Journal of Colloid and Interface Science*, vol. 308, no. 1, pp. 208–215, 2007.

[30] Y. H. Guo, C. W. Hu, S. C. Jiang, C. Guo, Y. Yang, and E. Wang, "Heterogeneous photodegradation of aqueous hydroxy butanedioic acid by microporous polyoxometalates," *Applied Catalysis B*, vol. 36, no. 1, pp. 9–17, 2002.

[31] E. B. Wang, C. W. Hu, and L. Xu, *Polyhydric Chemistry Introduction*, Chemical Industry Press, Beijing, China, 1998.